PERGAMON

Scripta Materialia 45 (2001) 781–786

Scripta MATERIALIA

www.elsevier.com/locate/scriptamat

Microstructural characterization of $(Fe_{0.5}Co_{0.5})_{88}Zr_7B_4Cu_1$ nanocrystalline alloys

D.H. Ping[a], Y.Q. Wu[a], K. Hono[a], M.A. Willard[b,1], M.E. McHenry[b], and D.E. Laughlin[b*]

[a]*National Institute for Materials Science, Sengen 1-2-1, Tsukuba 305-0047, Japan*

[b]*Department of Materials Science and Engineering, Carnegie Mellon University, Pittsburgh, PA 15213-3890, USA*

Received 17 April 2001; accepted 15 May 2001

Abstract

The distribution of Cu atoms in an $Fe_{44}Co_{44}Zr_7B_4Cu_1$ nanocrystalline alloy (HITPERM) has been studied by the three-dimensional atom probe technique. Cu atoms do not form clusters prior to the crystallization reaction, and they are partitioned in the remaining amorphous phase after crystallization. A Cu-free $Fe_{44.5}Co_{44.5}Zr_7B_4$ alloy has the same microstructure as the alloy with 1% Cu. © 2001 Acta Materialia Inc. Published by Elsevier Science Ltd. All rights reserved.

Keywords: Nanocrystalline; Soft magnetic; Microstructure; Atom probe; TEM

Introduction

Based on the Fe–Zr–B nanocrystalline soft magnetic alloys developed by Suzuki et al. [1], Willard et al. [2,3] recently developed a derivative nanocrystalline soft magnetic material for high temperature applications by replacing Fe with Co to a composition of $Fe_{44}Co_{44}Zr_7B_4Cu_1$. The crystallized microstructure is composed of nanoscale α'-FeCo particles (B2 structure) embedded in a residual amorphous phase. Since this soft magnetic material is intended to be used at a high temperatures (~550°C), they named this new alloy HITPERM. The room temperature AC permeability has been found to maintain a high value of 1800 up to a frequency of ~2 kHz. The core loss at room temperature is competitive with that of commercial high temperature alloys with a value of 1 W/g at $B_s = 10$ kG and $f = 1$ kHz. High magnetization persists to the $\alpha \rightarrow \gamma$ phase transformation temperature at 980°C.

* Corresponding author. Tel.: +1-412-268-2706; fax: +1-412-268-7169.

E-mail address: dl0p@andrew.cmu.edu (D.E. Laughlin).

[1] Present address: Naval Research Laboratory, Code 6342, 4555 Overlook Avenue, S.W. Washington, DC 20375-5343, USA.

PII: S1359-6462(01)01096-X

It is well known that the outstanding soft magnetic properties of FINEMET ($Fe_{73.5}Si_{13.5}B_9Nb_3Cu_1$) and NANOPERM ($Fe_{88}Zr_7B_4Cu_1$) are attributed to their nanocrystalline microstructures [1,4]. The mechanism of the nanocrystalline microstructure ?tul> evolution in these two alloys, in particular, the role Cu atoms play during the amorphous crystallization has been extensively studied by using the atom probe (AP) technique and high-resolution electron microscopy (HREM) [5–8]. The role of Cu additions in refining the nanocrystalline microstructure of Fe–Zr–B based soft magnetic alloys is now well established. Zhang et al. [7] clearly showed that Cu clusters form prior to the onset of the crystallization reaction of the $Fe_{89}Zr_7B_3Cu_1$ amorphous alloy using the atom probe technique. Recently, Ohkubo et al. [8] directly observed crystallographic orientation relationships between the Cu precipitate particles and α-Fe primary crystals using HREM and nanobeam diffraction techniques. In their work, 3DAP results also showed that Cu particles and α-Fe primary crystals are in direct contact with each other, suggesting that Cu precipitates act as heterogeneous nucleation sites for the α-Fe particles. On the other hand, Wu et al. [9] recently reported that the formation of Cu clusters is suppressed in Co containing Fe–Nd–B based alloys, while Cu clusters do form in Co-free Fe–Nd–B amorphous alloys.

In the HITPERM alloy, Cu was added as a nucleation agent from the beginning of the alloy design [10], and thus whether or not Cu is required for the formation of nanocrystalline microstructure has not been examined. As reported by Wu et al. [10], substantial additions of Co may influence the effect of Cu, and hence it is worthwhile examining whether or not Cu additions are essential for obtaining optimum soft magnetic properties in the HITPERM alloy. Hence, this work is aimed at understanding the clustering and/or partitioning behavior of Cu atoms during the crystallization process of an amorphous $Fe_{44}Co_{44}Zr_7B_4Cu_1$ alloy using the 3DAP technique.

Experimental procedure

The ingot, with a nominal composition of $Fe_{44}Co_{44}Zr_7B_4Cu_1$, was prepared by arc-melting pure elements (Fe, 99.9% with low C; Co, 99.9%; Zr, 99.9%; Fe_3B, 90.75%; metals basis and Cu, 99.99%) in an argon atmosphere. Amorphous ribbons were obtained by using a single roller melt spinning technique at a wheel surface velocity of 35 m/s. For comparison, a Cu-free alloy with a nominal composition of $Fe_{44.5}Co_{44.5}Zr_7B_4$ was also prepared. To obtain nanocrystalline microstructures, the as-quenched ribbons were isothermally annealed at 550°C for 1 h in an Ar atmosphere followed by water quenching. The ribbon shaped specimens were mechanically ground to square rods of approximately 20 μm × 20 μm × 6 mm and then sharpened by a micro-electropolishing technique to obtain field ion microscope (FIM) tip specimens. An energy compensated three-dimensional atom probe (EC-3DAP) equipped with the CAMECA optical tomographic atom probe (TAP) detection system [11] was used in this study. AP analyses were performed at a tip temperature of about 65 K in an ultrahigh vacuum condition ($< 1 \times 10^{-8}$ Pa) with a pulse fraction (a ratio of pulse voltage to the static voltage) of 0.2 and a pulse repetition rate of 600 Hz. A Philips CM200 TEM operated at 200 kV and a

HREM, JEOL JEM-4000EX with a point to point resolution of about 0.17 nm, was also used for microstructural characterization. TEM samples were prepared by ion milling.

Results and discussion

Fig. 1 shows a HREM image and corresponding selected area electron diffraction (SAED) pattern of the as-quenched $Fe_{44}Co_{44}Zr_7B_4Cu_1$ alloy. The isotropic maze pattern observed in the HREM image is a typical feature for an amorphous structure and hence indicates that the as-quenched ribbon sample is fully amorphous. No indication of fine crystallites has been observed by HREM observation. Fig. 2 shows 3DAP map of Cu atoms within a volume of $10 \times 10 \times 20$ nm^3 of the as-quenched sample, which reveals a uniform distribution of Cu atoms. We confirmed that the as-quenched Cu-free alloy was also fully amorphous with homogeneous distribution of all alloying elements.

The nanocrystalline microstructure is obtained by annealing the amorphous alloy at a temperature in the range of 510–700°C for 1 h [2]. Fig. 3 shows a bright field TEM micrograph and SAED pattern of (a) $Fe_{44}Co_{44}Zr_7B_4Cu_1$ and (b) Cu-free $Fe_{44.5}Co_{44.5}$-Zr_7B_4 amorphous alloys annealed at 550°C for 1 h. The SAED pattern indicates that the nanocrystals are randomly oriented bcc particles of ≈8 nm in diameter. However they have been identified as α′-(Fe, Co) phase with the B2 structure by synchrotron X-ray diffraction [2,3]. It is difficult to see the superlattice diffraction rings of the B2 structure from the electron diffraction pattern because of the similarity of the atomic scattering factors of Fe and Co as well as the small particle size. The {0 1 1} diffraction ring overlaps with the weak halo of the amorphous phase, indicating that some intergranular amorphous phase remains in this stage. It should be noted that the contrast from the nanograins suggests that the nanograins are not completely randomly oriented, but groups of several grains show dark contrast suggesting that these grains are similarly oriented (satisfying the same diffraction condition). These microstructural

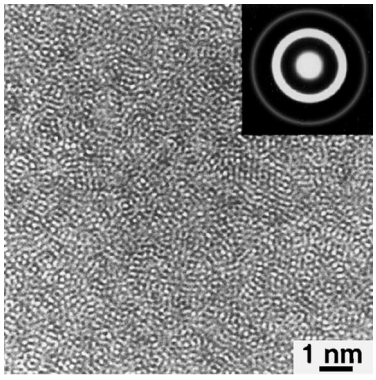

1

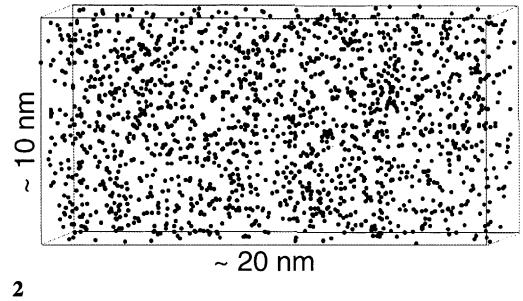

2

Fig. 1. HREM image and corresponding SAED pattern of the as-quenched $Fe_{44}Co_{44}Zr_7B_4Cu_1$ alloy.

Fig. 2. 3DAP elemental mapping of Cu in the as-quenched $Fe_{44}Co_{44}Zr_7B_4Cu_1$ alloy. The Cu atoms are uniformly distributed.

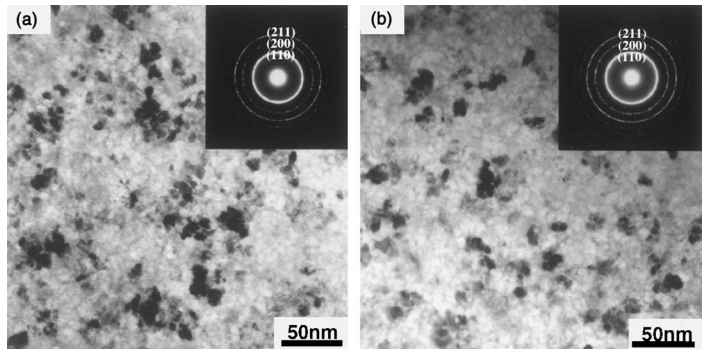

Fig. 3. Bright field micrographs and SAED patterns of the (a) $Fe_{44}Co_{44}Zr_7B_4Cu_1$ alloy and (b) $Fe_{44.5}Co_{44.5}Zr_7B_4$ alloy annealed at 550°C for 60 min. There is no obvious difference of the average grain size between those two alloys.

features are very similar to the ones observed in the $Fe_{86}Zr_7B_6$ alloy observed by Suzuki et al. [1]. They observed that nanograins are more randomly oriented in the $Fe_{86}Zr_7B_6Cu_1$ alloy. On the other hand, both Fig. 3(a) and (b) show similar microstructural features, suggesting that the presence of Cu does not have much influence on the microstructure.

The partitioning behavior of the alloying elements in the above sample can be seen clearly from 3DAP elemental maps. Fig. 4 is the 3DAP analysis result of the $Fe_{44}Co_{44}Zr_7B_4Cu_1$ alloy annealed at 550°C for 1 h. Fig. 4(a) shows the elemental distributions of Zr and Cu atoms in a volume of $6 \times 6 \times 40$ nm^3. The black dots in each map represent the positions of the alloying elements. The Zr-enriched regions correspond to the residual amorphous phase and the Zr-depleted areas are the α'-(Fe, Co) grains. Unlike the 3DAP results from the $Fe_{88}Zr_7B_4Cu_1$ alloys [2], neither Cu clusters nor precipitates can be observed from the Cu elemental map of the HITPERM alloy. The Co, Zr, B and Cu atoms are found to partition preferentially into the residual amorphous phase. In order to evaluate quantitatively the partitioning behavior of the alloying elements, integrated concentration depth profiles (ladder diagrams) determined from the selected volume are shown in Fig. 4(b). The α'-(Fe, Co) grains contain about 58 at.%Fe, 37 at.%Co, 1 at.%Zr and 3 at.%B on average. Cu atoms are partitioned in the residual amorphous phase. No Cu clusters or Cu crystalline particles were detected in this stage. Co atoms are not uniformly distributed in the alloy, the amorphous regions are slightly enriched Co. Thus, the α'-(Fe, Co) phase is slightly rich in Fe, having a Fe:Co atomic ratio of $\sim$1.5. The composition of the amorphous phase is close to 34.5%Fe, 49.0%Co, 10.0%Zr, 4.8%B, and 1.7%Cu.

Cu is known to form clusters prior to the crystallization of $Fe_{89}Zr_7B_3Cu_1$ amorphous alloys. Since Fe and Co both have small solubility with Cu, it was anticipated that substitution of Co for Fe would not greatly change the solubility of Cu in the master alloy. Therefore, it is surprising to find that the Cu atoms do not form clusters in the Co containing alloy. A similar phenomenon was noticed in the Co-containing nanocomposite α-Fe/$Nd_2Fe_{14}B$ hard magnetic alloys [9]. This might be due to the change in the driving force for phase separation in the amorphous phase. The enthalpy of mixing

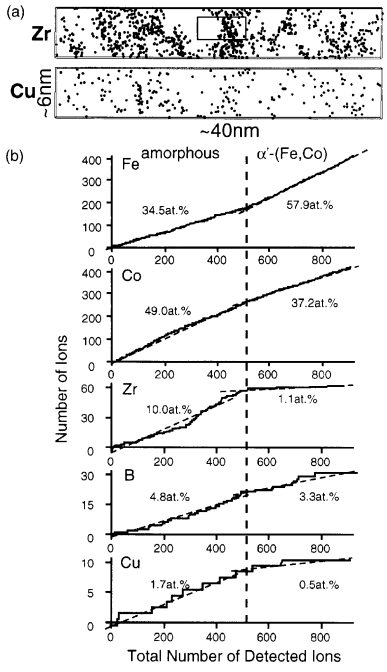

4

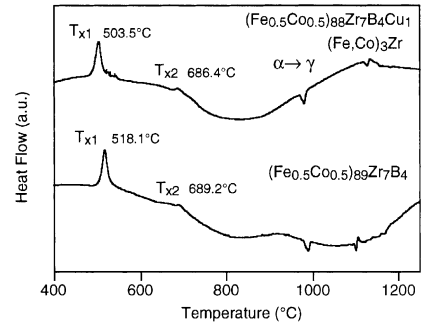

5

Fig. 4. 3DAP results of the $Fe_{44}Co_{44}Zr_7B_4Cu_1$ nanocrystalline alloy annealed at 550°C for 60 min. (a) Zr and Cu mappings detected in the volume of $6 \times 6 \times 40$ nm^3. The Zr-depleted regions correspond to the α′-(Fe, Co) particles. (b) Integral concentration profiles of Fe, Co, Zr, B and Cu obtained from the selected volume. Co, Zr, B and Cu are rejected from the α′-(Fe, Co) particles and partitioned into residual amorphous phase.

Fig. 5. DTA results of the (a) $Fe_{44}Co_{44}Zr_7B_4Cu_1$ and (b) $Fe_{44.5}Co_{44.5}Zr_7B_4$ alloys at a scanning rate of 0.167°C/s.

between Fe and Cu is 50 kJ/mol, while that for Co and Cu is 25 kJ/mol [12]. Thus, it is concluded that Fe and Cu are more mutually repulsive than Co and Cu. Since the driving force for cluster formation of Cu is phase separation of Cu from the amorphous solid solution, by replacing Co for Fe, the driving force for the phase separation decreases as the enthalpy of mixing of Cu within the matrix phase decreases. This could be the reason why Cu clusters do not form in the HITPERM alloy. It should also be noticed that the enthalpy of mixing for Co and Zr is very negative, −197 kJ/mol, while that for Fe and Zr is −118 kJ/mol. This suggests that Co and Zr are more attractive. Because of this, Co is weakly enriched in the remaining phase rather than enriched in the α′-(Fe, Co) solid solution.

Since Cu atoms do not form clusters, they do not provide heterogeneous nucleation sites for the α′-(Fe, Co) primary crystals. In fact, no obvious difference in the grain sizes can be seen in the two alloys (Cu-containing and Cu-free alloys) annealed at 550°C for 1 h as shown in Fig. 3. Thus Cu additions do not seem to have an influence in reducing the grain size in the HITPERM alloy. This suggests that Cu can be omitted from the HITPERM alloy, which has the benefit of increasing the saturation magnetic flux density. The coercivities measured from both the alloys were almost the same, 0.3 Oe. Although Cu additions do not influence the microstructure (or coercivities), Cu

additions do change the crystallization temperature. Fig. 5 are the results of differential thermal analysis (DTA) of the Cu-containing and Cu-free samples at a heating rate of 0.167°C/s. Two distinct crystallization events (T_{x1} and T_{x2}, which correspond to the crystallization of α'-(Fe, Co) and $(Fe, Co)_3$ Zr, respectively) were observed. The Cu addition reduces the crystallization temperature of the α'-(Fe, Co) phase from ~518.1°C to 503.5°C. The decrease of the crystallization temperatures as a result of Cu addition to Fe-based amorphous alloys have been commonly observed [1,4]. This has been interpreted as a result of the nucleation catalysis effect due to the presence of Cu clusters. Since Cu clusters do not form in the HITPERM alloy, the reduction of the T_x by Cu addition may be attributed to the decrease in the melting temperature of the alloy by Cu addition.

Conclusions

The microstructural evolution of soft magnetic $Fe_{44}Co_{44}Zr_7B_4Cu_1$ alloy (HITPERM) has been studied by using 3DAP and TEM and compared with that of a Cu-free $Fe_{44.5}Co_{44.5}Zr_7B_4$ alloy. Cu atoms do not form clusters prior to the crystallization reaction in this alloy composition. No difference was observed in the final microstructures of the Cu-containing and Cu-free alloys. Cu atoms are partitioned in the remaining amorphous phase. Thus, Cu is not a required element in the HITPERM alloy.

Acknowledgements

This work was partly supported by the special coordination fund for Promoting Science and Technology on "Nanohetero Metallic Materials" from the Science and Technology Agency. The CMU effort was sponsored by the Air Force Office of Scientific Research, Air Force Materiel Command, USAF, under grant number F49620-96-1-0454.

References

[1] Suzuki, K., Makino, A., Kataoka, N., Inoue, A., & Masumoto, T. (1991). Mater Trans JIM 32, 93.
[2] Willard, M. A., Laughlin, D. E., Mchenry, M. E., Thoma, D., Sickafus, K., Cross, J. O., & Harris, V. G. (1998). J Appl Phys 84, 6773.
[3] Willard, M. A., Huang, M. Q., Laughlin, D. E., Mchenry, M. E., Cross, J. O., Harris, V. G., & Franchetti, C. (1999). J Appl Phys 85, 4421.
[4] Yoshizawa, Y., & Yamauchi, K. (1990). Mater Trans JIM 21, 307.
[5] Hono, K., Hiraga, K., Wang, Q., Inoue, A., & Sakurai, T. (1992). Acta Metall Mater 40, 2137.
[6] Hono, K., Ping, D. H., Ohnuma, M., & Onodera, H. (1999). Acta Mater 47, 997.
[7] Zhang, Y., Hono, K., Inoue, A., & Sakurai, T. (1996). Mater Sci Eng A 217/218, 407.
[8] Ohkubo, T., Kai, H., Ping, D. H., Hono, K., & Hirotsu, Y. (2001). Scripta Mater 44, 971.
[9] Wu, Y. Q., Ping, D. H., Hono, K., Hamano, M., & Inoue, A. (2000). J Appl Phys 87, 8658.
[10] McHenry, M. E., Willard, M. A., & Laughlin, D. E. (1999). Prog Mater Sci 44, 291.
[11] Deconihout, B., Renaud, L., Da Costa, G., Bouet, M., Bostel, A., & Blavette, D. (1998). Ultramicroscopy 73, 253.
[12] Bakker, H. (1998). Enthalpies in Alloys – Miedema's Semi-Empirical Model. Zülich: Trans Tech Publications.